

Nonlinear saturable absorption of vertically stood WS₂ nanoplates

Xiuli Fu,^{1,*} Jingwen Qian,^{1,2} Xiaofen Qiao,³ Pingheng Tan,³ and Zhijian Peng^{2,4}

¹State Key Laboratory of Information Photonics and Optical Communications, and School of Science, Beijing University of Posts and Telecommunications, Beijing 100876, China

²School of Engineering and Technology, China University of Geosciences, Beijing 100083, China

³State Key Laboratory of Superlattices and Microstructures, Institute of Semiconductors, Chinese Academy of Sciences, Beijing 100083, China

⁴e-mail: pengzhijian@cugb.edu.cn

*Corresponding author: xiulifu@bupt.edu.cn

Received August 13, 2014; revised September 23, 2014; accepted October 14, 2014;
posted October 15, 2014 (Doc. ID 220864); published November 10, 2014

We report the nonlinear optical (NLO) properties of vertically stood WS₂ nanoplates excited by 532-nm picosecond laser light. The nanoplates were synthesized by a no-catalyst thermal evaporation process. Raman spectroscopy and x-ray diffraction pattern indicate that the nanoplates are of high crystal quality. The nanoplates exhibit large nonlinear saturable absorption but negligible nonlinear refraction. Mechanisms of the NLO response are proposed. © 2014 Optical Society of America

OCIS codes: (190.4720) Optical nonlinearities of condensed matter; (160.4236) Nanomaterials; (190.5650) Raman effect.

<http://dx.doi.org/10.1364/OL.39.006450>

Since the discovery of graphene, layered transition metal dichalcogenides (TMDCs) have attracted growing attention, owing to their remarkable electrical and optical properties with intriguing potential in optoelectronic applications [1–4]. Tungsten disulfide (WS₂) is one of those layered TMDCs. In its bulk form, WS₂ is a semiconductor with direct band-gap of 1.95 eV and indirect band-gap of 2.36 eV [5]. It has been exploited in catalysis, field-effect transistors, lithium ion batteries, and so on [6–9]. But so far, its applicability in photonics and optoelectronics is less studied. As is well known, the development of viable photonic devices primarily depends on materials with remarkable specific optical properties, such as luminescence, optical limiting, and so forth [3,10,11]. Unfortunately, bulk WS₂ crystals or conventionally deposited WS₂ thin films possess no such properties, limiting the range of their use, for instance, in photonics [12,13].

Bulk WS₂ is composed of covalently bonded S-W-S planes, forming two-dimensional (2D) layers that are bonded together by van der Waals forces, which are weak, allowing the layers to form robust 2D nanostructures similar to graphite nanoclusters. Due to specific 2D confinement of electron motion and an absence of inter-layer coupling, single-layer WS₂ possesses a direct band gap, making its light emission dramatically better than that of its bulk counterpart [12,14]. For example, a monolayer WS₂ flake mechanically exfoliated from a synthetic bulk crystal exhibits uniform photoluminescence (PL) [12]. Extraordinary PL near the edge of triangular WS₂ clusters grown by CVD was reported in Ref. [14]. Here, we report our detailed experimental investigation on the ultrafast nonlinear response of WS₂ nanoplates prepared by a no-catalyst thermal evaporation process. To shed more light on the underlying physical mechanisms of their nonlinear optical (NLO) response, experiments were conducted using visible (532 nm) and infrared (1064 nm), picosecond laser pulses at different excitation

intensities. In addition, the crystal quality of the WS₂ nanoplates was verified by polarized micro-Raman spectra and compared with the bulk WS₂.

The WS₂ nanoplate synthesis process was reported elsewhere in detail [15]. Figure 1(a) is a typical image of a large quantity of the WS₂ nanostructures from field-emission scanning electron microscopy (SEM). In the high-magnification SEM image shown in Fig. 1(b), a rod-like feature is observed from the top view because the nanostructures are aligned in a very dense array that is approximately perpendicular to the substrate surface. The array appears to cover the substrate quite uniformly, judging from the SEM images. To determine the

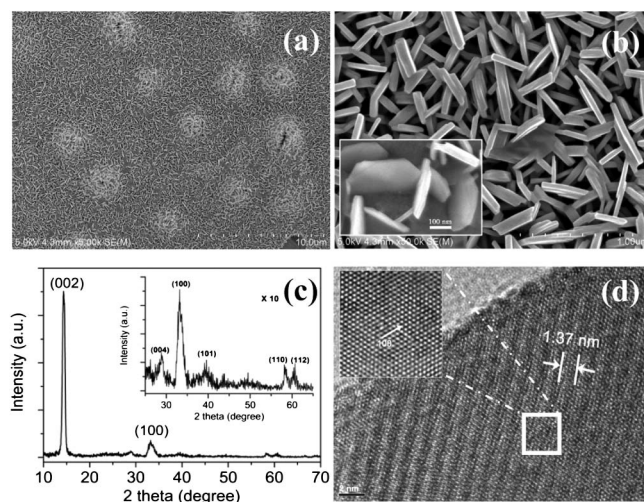


Fig. 1. (a) Low-magnification and (b) high-magnification SEM images of the nanoplates. The SEM image in the inset (b) was taken under a tilted scan angle. (c) Typical XRD pattern of the WS₂ nanoplates, in which all the diffraction peaks can be assigned to pure 2H (hexagonal) WS₂. (d) HRTEM of a single nanoplate.

morphology of the nanostructure, a typical SEM image, taken under a tilted scan angle, of several nanostructures is shown in the inset of Fig. 1(b), clearly displaying a well-defined plate-like morphology of the nanostructure. And it was measured that the width of the plates is in the range of 200–300 nm. By examining tens of the WS₂ nanoplates, it was found that their thickness is in the range of 20–30 nm. X-ray diffraction (XRD) patterns of the nanoplates are shown in Fig. 1(c). All the diffraction peaks were indexed to the hexagonal phase of WS₂ (2H-WS₂). The intense (001) diffraction reveals good crystallinity of the nanoplates, and the high intensity of the (002) diffraction of the *c* axis reflects the vertical arrangement of the nanoplates. Figure 1(d) is a representative image from high-resolution transmission electron microscopy (HR-TEM), showing a good agreement with the XRD observations [Fig. 1(c)]. The light and dark stripes observed in a single nanoplate confirm its layered structure. The well-resolved periodic lattice fringe, clearly shown in the inset, further reveals the well-crystallized single-crystal nature of these WS₂ nanoplates. Based on the measured spacing of dark fringes (about 1.37 nm), the calculated thickness of the nanoplates is approximately 20.49 nm, which is almost equal to the SEM result.

Raman spectroscopy was employed to confirm the atomic structural arrangement of the WS₂ nanoplates along with bulk WS₂ for comparison under VH and VV polarization configurations, as shown in Fig. 2. Here, VH (VV) means that the incident light is perpendicular (parallel) to the scattered light. The measurement was carried out using a Jobin Yvon HR800 Raman spectrometer with a laser at 532 nm. A typical laser power of 0.1 mW was used in order to avoid sample heating. As previously reported [16–18], the first-order Raman spectra of bulk WS₂ in the backscattering geometry show two optical phonon modes (E_{2g}^1 at 356 cm⁻¹ and A_{1g} at 421 cm⁻¹) and one longitudinal acoustic mode (LA(M) at 176 cm⁻¹), where E_{2g}^1 is an in-plane optical mode and A_{1g} corresponds to the out-of-plane vibrations along

the *c* axis direction of the sulfur atoms. Notably, the E_{2g}^1 and A_{1g} peaks are observed in parallel polarization, while only E_{2g}^1 peak appears in cross-polarization, similar to the polarization dependence of the corresponding modes in multilayer and bulk MoS₂ [19]. Indeed, as determined by the Raman tensors of E_{2g}^1 and A_{1g} [19], E_{2g}^1 is present in two polarization configurations, while the mode A_{1g} is allowed only under parallel polarization in the back-scattering configuration. The peak at 175 cm⁻¹ is identified as an LA phonon at the M point, and the broad peak at 351 cm⁻¹ is assigned as its second-order phonon 2LA (M) [20]. The other weak peaks at 193, 231, 312, and 324 cm⁻¹, labeled by stars (*), are second-order Raman modes [20].

As for the present vertically standing WS₂ nanoplates, the positions of all the observed Raman bands are in good agreement with those in bulk WS₂, evidencing that the quality levels of both the crystallinity and the lattice are comparable with that of bulk crystal. The new peak at 383 cm⁻¹ may be from the multiphonon modes at the Brillouin zone edge [20]. The absolute intensity of the main Raman peaks [2LA(M), E_{2g}^1 , and A_{1g}] changes sharply. For example, the E_{2g}^1 mode is about 2 times stronger than A_{1g} for bulk WS₂, and the E_{2g}^1 mode of the nanoplates is overshadowed by the presence of the high-intensity 2LA(M) phonon mode with only half as intense as the A_{1g} mode. Such a behavior could be attributed to a higher scattering volume along *c* axis of the nanoplates. It must be pointed out that the strong A_{1g} mode is observed in the spectrum of orthotropic WS₂ nanoplates under both VV and VH measurement configurations, showing no obvious dependence on polarization. In principle, for an individual vertically standing WS₂ nanoplate, A_{1g} mode is forbidden in cross-(VH) polarization configuration if the polarization direction of the laser is along the *c* axis. This phenomenon observed in this study is due to the random distribution of the *c* axis for the investigated WS₂ nanoplates. The angle between the polarization direction of the laser and the *c* axis can be varied from 0 to 90 deg so that A_{1g} phonon can be observed under both VV and VH configurations.

The NLO properties of WS₂ nanoplates transferred onto a quartz substrate were investigated by an open-aperture (OA) z-scan system in conjunction with a picosecond Nd:YAG laser operating at 532 nm, 25 ps pulses, with 10 Hz repetition rate. The incident and transmitted laser powers were monitored as the sample was moved (or *z* scanned) along the propagation direction of laser pulses. Figure 3(a) shows some typical OA z-scans carried out at different incident laser intensities. As shown, the NLO response of WS₂ nanoplates took place when the excitation energy was increased to 0.20 GW/cm². At excitation energies larger than 0.75 GW/cm², the WS₂ nanoplates exhibit a significant saturable absorption (SA) response, similar to that of monolayer and few-layer MoS₂ nanosheets for the femtosecond pulses at 800 nm [21]. That is, the total transmission increases with greater intensity of the incident beam, the maximum being at the beam focus.

To quantitatively determine the SA properties of the present WS₂ nanoplates, the corresponding Z-scan data were simulated [22]. In the model the optical intensity

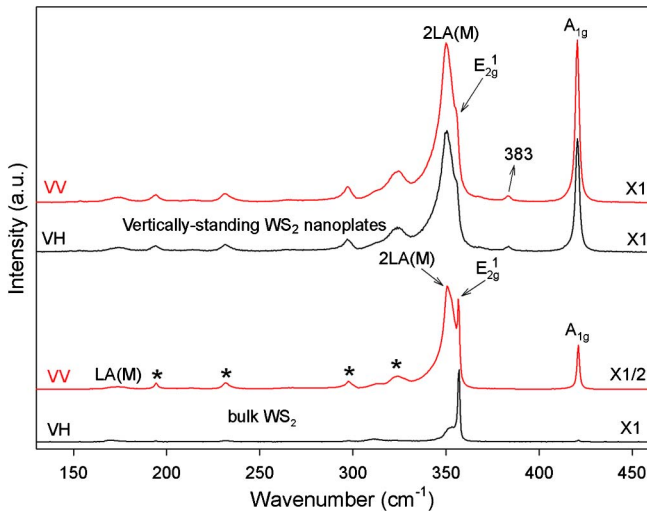


Fig. 2. Raman spectra of bulk WS₂ and the present vertically standing WS₂ nanoplates under VH and VV configurations, where VH (VV) means that the incident light is perpendicular (parallel) to the scattered light.

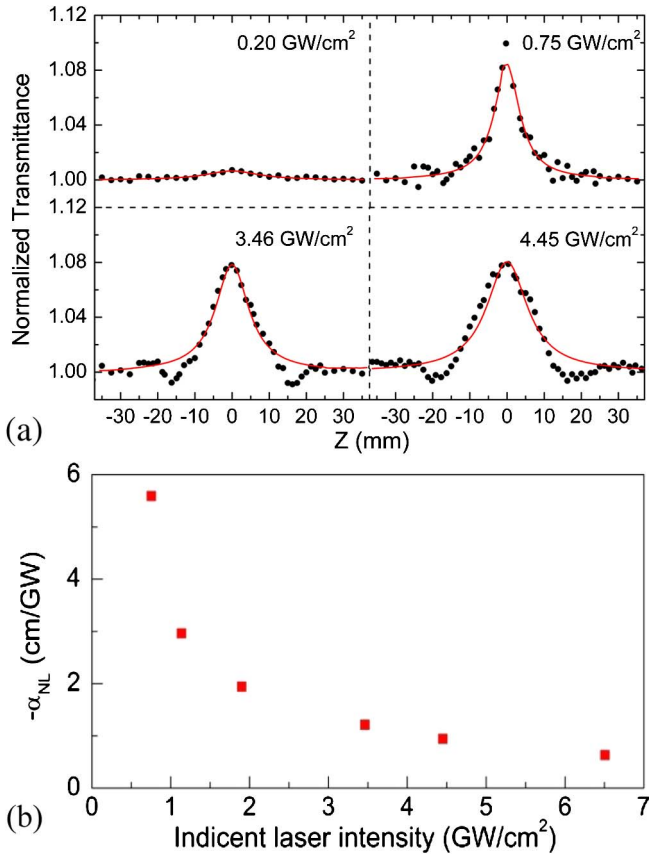


Fig. 3. (a) Open-aperture Z-scans of the WS₂ nanoplates on quartz substrate obtained under 25-ps, 532-nm laser excitation. The solid lines represent the best fits of the experimental data. (b) The measured nonlinear absorption coefficient (α_{NL}) values versus the incident laser intensity of the nanoplates.

loss, as the beam propagates through the “thin” sample, is given by the relation

$$dI/dz = -\alpha(I) * I, \quad (1)$$

where z is the propagation distance, I is the intensity of the laser beam within the sample, and $\alpha(I)$ is the intensity dependent absorption coefficient given by

$$\alpha(I) = \alpha_0 + \alpha_{NL}I, \quad (2)$$

where α_0 is the linear absorption coefficient at the excitation wavelength, and α_{NL} is a nonlinear absorption coefficient, which is proportional to the imaginary part of third-order nonlinear susceptibility. Following Eqs. (1) and (2), the normalized power transmittance can be calculated as a function of z -position of the sample using α_{NL} as a free parameter. The α_{NL} can be extracted from the best fitting curve. The solid line in Fig. 3(a) shows the best fit to experimental z-scan data at each laser intensity. The obtained α_{NL} of the nanoplates have values of -5.59 , -2.96 , -1.94 , -1.21 , -0.94 , and -0.63 cm/GW, respectively, as the incident laser intensity changes from 0.75 to 6.51 GW/cm², e.g., 0.75, 1.14, 1.90, 3.46, 4.45, and 6.51 GW/cm². It was found that the measured value decreases monotonously as the laser intensity increases, as shown in Fig. 3(b), implying that there are no two-photon

absorption effects. Note that one cannot observe a clear nonlinear response from the quartz substrate in any of the experiments, meaning that the contribution of α_{NL} comes only from the nonlinear absorption of the WS₂ nanoplates. In addition, during the present experiments, the WS₂ nanoplates exhibit no measurable nonlinear refraction under any of the employed excitation conditions, suggesting that there might be no nonlinear refraction or that it is lower than the detection limits of the applied equipment, and/or that it might have been greatly suppressed owing to the strong nonlinear absorption. Taking into account the measured band-gap of ~ 1.85 eV from the UV-vis absorption spectrum of WS₂ nanoplates, the bleaching of the ground-state absorption arising from a strong one-photon absorption process [23] is a plausible mechanism to explain the form of the obtained OA Z-scans under 532 nm (i.e., ~ 2.34 eV) excitation.

Similar z-scan measurements (not shown here) were also performed under 1064-nm (i.e., ~ 1.16 eV), 25-ps laser excitation, recording an identical but very weak NLO response only for incident intensities up to 9.60 GW/cm², which could be attributed to the formation of localized defect states or surface states induced by the high excitation intensity applied. As reported in Refs. [24–26], the defect centers in semiconductor nanocrystals, which may act as photon-trapping states over the surface, are responsible for the optical nonlinear properties. To be specific, if the linear absorption cross-section of the trap states is higher than that of the ground state, the direct excitation from these surface-trapped states will promote the photocarriers to higher energy levels in the nanocrystal, giving rise to the optical nonlinearity. Such a situation is also supported by the OA z-scans obtained under 532 nm excitation. From Fig. 3(a), it is clearly seen that, when the incident laser intensity increased up to 3.46 GW/cm², the OA z-scan curves could not be successfully fitted using the absorption coefficient described by Eq. (2), in which two valleys (decreased transmittances) appear near the peak. We propose that this change in the nonlinear behavior is related to the changes in defect state density.

In conclusion, we have systematically investigated the Raman behavior and nonlinear saturable absorption properties of the synthesized well-arranged WS₂ nanoplates. The Raman measurements reveal that the E_{2g}^1 Raman mode of the WS₂ nanoplates softens, while the 2LA(M) and A_{1g} modes present a hardening that is much more subtle than in bulk WS₂. The WS₂ nanoplates exhibit distinct NLO response during OA z-scan measurements at different incident laser excitations. Under all the experimental conditions employed in this study, the WS₂ nanoplates present only nonlinear saturable absorption, while nonlinear refraction is absent, indicating that the WS₂ nanoplates can effectively suppress low intensity light but allow the high intensity light to pass. The present WS₂ nanoplates are promising 2D nanomaterials for nanophotonic devices, such as saturable absorbers and optical switches.

The authors would like to thank the financial support for this work from the National Natural Science Foundation of China (Grant Nos. 11274052, 51172030, 61274015,

11474277, 11434010, and 11225421), Excellent Adviser Foundation in China University of Geosciences from the Fundamental Research Funds for the Central Universities, and National Basic Research Program of China (Grant No. 2010CB923200).

References

1. A. H. C. Neto and K. Novoselov, *Rep. Prog. Phys.* **74**, 82501 (2011).
2. Q. H. Wang, K. Kalantar-Zadeh, A. Kis, J. N. Coleman, and M. S. Strano, *Nat. Nanotechnol.* **7**, 699 (2012).
3. S. Z. Butler, S. M. Hollen, L. Cao, Y. Cui, J. A. Gupta, H. R. Gutiérrez, T. F. Heinz, S. S. Hong, J. Huang, A. F. Ismach, E. Johnston-Halperin, M. Kuno, V. V. Plashnitsa, R. D. Robinson, R. S. Ruoff, S. Salahuddin, J. Shan, L. Shi, M. G. Spencer, M. Terrones, W. Windl, and J. E. Goldberger, *ACS Nano* **7**, 2898 (2013).
4. M. Chhowalla, H. S. Shin, G. Eda, L. Li, K. P. Loh, and H. Zhang, *Nat. Chem.* **5**, 263 (2013).
5. A. Klein, S. Tiefenbacher, V. Eyert, C. Pettenkofer, and W. Jaegermann, *Phys. Rev. B* **64**, 205416 (2001).
6. D. Voiry, H. Yamaguchi, J. Li, R. Silva, D. C. B. Alves, T. Fujita, M. Chen, T. Asefa, V. B. Shenoy, G. Eda, and M. Chhowalla, *Nat. Mater.* **12**, 850 (2013).
7. T. Georgiou, R. Jalil, B. D. Belle, L. Britnell, R. V. Gorbachev, S. V. Morozov, Y. J. Kim, A. Gholinia, S. J. Haigh, O. Makarovskiy, L. Eaves, L. A. Ponomarenko, A. K. Geim, K. S. Novoselov, and A. Mishchenko, *Nat. Nanotechnol.* **8**, 100 (2012).
8. R. Bhandavat, L. David, and G. Singh, *J. Phys. Chem. Lett.* **3**, 1523 (2012).
9. J. Yang, D. Voiry, S. J. Ahn, D. Kang, A. Y. Kim, M. Chhowalla, and H. S. Shin, *Angew. Chem., Int. Ed.* **52**, 13751 (2013).
10. F. Bonaccorso, Z. Sun, T. Hasan, and A. C. Ferrari, *Nat. Photonics* **4**, 611 (2010).
11. K. P. Loh, Q. L. Bao, G. Eda, and M. Chhowalla, *Nat. Chem.* **2**, 1015 (2010).
12. H. L. Zeng, G. B. Liu, J. F. Dai, Y. J. Yan, B. R. Zhu, R. C. He, L. Xie, S. J. Xu, X. H. Chen, W. Yao, and X. D. Cui, *Sci. Rep.* **3**, 1608 (2013).
13. A. H. Reshaka and S. Auluck, *Physica B* **393**, 88 (2007).
14. H. R. Gutiérrez, N. Perea-López, A. L. Elías, A. Berkdemir, B. Wang, R. Lv, F. López-Urías, V. H. Crespi, H. Terrones, and M. Terrones, *Nano Lett.* **13**, 3447 (2013).
15. J. W. Qian, Z. J. Peng, D. Z. Wu, and X. L. Fu, "Simple large-scale synthesis of WS₂ nanoplates," submitted to *Dalton Trans.*
16. J. L. Verble, *Phys. Rev. Lett.* **25**, 362 (1970).
17. C. Sourisseau, F. Cruege, M. Fouassier, and M. Alba, *Chem. Phys.* **150**, 281 (1991).
18. R. Loudon, *Adv. Phys.* **50**, 813 (2001).
19. X. Zhang, W. P. Han, J. B. Wu, S. Milana, Y. Lu, Q. Q. Li, A. C. Ferrari, and P. H. Tan, *Phys. Rev. B* **87**, 115413 (2013).
20. W. J. Zhao, Z. Ghorannevis, K. K. Amara, J. R. Pang, M. Toh, X. Zhang, C. Kloc, P. H. Tan, and G. Eda, *Nanoscale* **5**, 9677 (2013).
21. K. P. Wang, J. Wang, J. T. Fan, M. Lotya, A. O'Neill, D. Fox, Y. Y. Feng, X. Y. Zhang, B. X. Jiang, Q. Z. Zhao, H. Z. Zhang, J. N. Coleman, L. Zhang, and W. J. Blau, *ACS Nano* **7**, 9260 (2013).
22. M. Sheik-Bahae, A. A. Said, T. H. Wei, D. J. Hagan, and E. W. Van Stryland, *IEEE J. Quantum Electron.* **26**, 760 (1990).
23. H. S. Nalwa, *Handbook of Nanostructured Materials and Nanotechnology* (Academic, 2000).
24. P. A. Kurian, C. Vijayan, C. S. S. Sandeep, R. Philip, and K. Sathiyamoorthy, *Nanotechnol.* **18**, 075708 (2007).
25. D. J. Asunsakis, I. L. Bolotin, J. E. Haley, A. Urbas, and L. Hanley, *J. Phys. Chem. C* **113**, 19824 (2009).
26. N. Illyaskutty, S. Sreedhar, H. Kohler, R. Philip, V. Rajan, and V. P. M. Pillai, *J. Phys. Chem. C* **117**, 7818 (2013).